Available online at www.sciencedirect.com

SCIENCE DIRECT®

Catalysis Today 93–95 (2004) 603–606

CATALYSIS TODAY

www.elsevier.com/locate/cattod

Study on catalytic hydrogenation properties and thermal stability of amorphous NiB alloy supported on carbon nanotubes

Minwei Wang[a], Fengyi Li[b,*], Rongbin Zhang[b]

[a] *Department of Chemical Engineering, Nanchang University, Nanchang 330029, China*
[b] *Institute of Applied Chemistry, Nanchang University, Nanchang 330047, China*

Abstract

The supported amorphous NiB/CNTs catalyst was prepared by impregnation, following the chemical reduction with KBH_4 solution. The gas-phase benzene hydrogenation was used as a probe reaction to evaluate the catalytic activity. The amorphous NiB/CNTs catalyst exhibited higher activity than the amorphous NiB/γ-Al_2O_3 catalyst. The difference in activity was due to the better dispersion of active nickel and the electronic interaction between Ni and CNTs on the NiB/CNTs catalyst. The thermal stability of amorphous NiB/CNTs was better than that of NiB/γ-Al_2O_3. Because the unique pore-channel structure of CNTs can protect the active component Ni against agglomeration. Such results were discussed based on various characterizations, including XRD, ICP, XPS, TEM, DSC and CO chemical adsorption.

Keywords: Amorphous alloy; Carbon nanotubes (CNTs); Thermal stability

1. Introduction

Amorphous alloys have received more attention from catalysis researchers since 1980s. It is proved [1–4] that amorphous alloys exhibit higher catalytic activity than corresponding crystalline catalyst. However, the extremely poor thermal stability, which results from the agglomeration of ultrafine amorphous alloy particles, limits their practical applications. Carbon nanotubes (CNTs), as a new kind of catalytic material with unique structure and properties, have received more attention [5–8]. In our study, we find that the electronic properties of CNTs promote the activity of catalyst obviously and the unique pore-channel structure can protect the active component against agglomeration. Hence the thermal stability of amorphous NiB/CNTs is improved.

2. Experimental

2.1. Catalyst preparation

The amorphous NiB/CNTs and NiB/γ-Al_2O_3 catalysts were prepared by following procedures. The CNTs support was synthesized and purified by the known method [9]. A desired amount of support was impregnated with an ethanol solution of 1 M $Ni(NO_3)_2{\cdot}6H_2O$ overnight. The mixture was reduced by adding dropwise several milliliters of KBH_4 aqueous solution under vigorous stirring at room temperature. The black precipitate, formed in the process of reaction, was washed with aqueous ammonia first after the reaction ceased, then with distilled water, followed by ethanol in order to remove some water-soluble impurities. Finally, the precipitate was dried at room temperature under the protection of pure nitrogen flow.

2.2. Catalyst characterization

The Ni-loading on the support were analyzed by means of inductively coupled plasma (ICP). The surface area of active nickel (S_{Ni}) was determined by CO chemical adsorption [9]. The amorphous characteristics of the as-prepared samples were investigated by X-ray diffraction (XRD) performed on a D/max-IIIA polycrystalline X-ray instrument under these conditions: target, Cu Kα; voltage, 30 kV; current, 30 mA; scan speed, $4^\circ\ min^{-1}$.

The X-ray photoelectron spectrometry (XPS) was performed on a VG ESCA-LAB MARK II X-ray photoelectron spectrometer under these conditions: target, Mg Kα; voltage, 12 kV; current, 20 mA. The differential scanning calorimetry

---

[*] Corresponding author. Tel.: +86 791 8305822.
E-mail addresses: annwang2@163.com (M. Wang), fy-li@sohu.com (F. Li).

0920-5861/$ – see front matter © 2004 Elsevier B.V. All rights reserved.
doi:10.1016/j.cattod.2004.06.012

(DSC) was performed on Perkin-Elmer DSC-2C differential scanning calorimeter. The TEM observations were performed by using a Hitachi-600 transmission electron microscope.

2.3. Evaluation of catalytic activity

The hydrogenation of benzene was applied to evaluate the catalytic activity. The hydrogenation reaction was carried out in a micro-reactor (stainless steel U-shape tube, 4 mm i.d.) under atmospheric pressure. Hydrogen was employed as reductive gas and carrier gas. The catalyst was reduced in situ at 473 K for 1 h before the reaction was performed. A volume of 1 μl benzene was injected into the reactor containing 0.1 g catalyst each time. The product and reactant were analyzed by an on-line gas chromatograph equipped with TCD and data integration.

3. Results and discussion

The Ni-loading on the support and the active nickel surface areas of the fresh catalysts are listed in Table 1. From Table 1, we can observe that the Ni-loading on the amorphous NiB/CNTs alloys is obviously smaller than that on the amorphous NiB/γ-Al_2O_3, although the same amount of nickel nitrate solution is used in the process of preparation. Compared to traditional support, such as Al_2O_3, CNTs exhibit hydrophobic character. The hydrophobicity of the surface maybe influences the process of reduction reaction when preparing the amorphous NiB alloy, which should be further studied. However, the S_{Ni} of amorphous NiB/CNTs is distinctively higher than that of amorphous NiB/γ-Al_2O_3, as shown in Table 1. This result shows that active nickel is dispersed well on CNTs than on γ-Al_2O_3 and more active sites exist on the surface of amorphous NiB/CNTs catalyst.

Table 2 summarizes the catalytic activity of different catalysts at different reaction temperature. Clearly, the activity of amorphous NiB/CNTs is obviously higher than that of amorphous NiB/γ-Al_2O_3 catalyst, especially at low reaction temperature. One reason is that there are more active sites on the surface of amorphous NiB/CNTs catalyst as mentioned above. The excellent electronic properties of CNTs also play an important role in benzene hydrogenation. It has been reported that [10] carbon nanotubes, as one kind of allotrope of carbon, are evolved from graphite. Therefore, there are a lot of moving single electrons on the wall of CNTs which makes CNTs has strong ability of losing electron. According to the results of XPS in Table 3, we can also find that electrons transfer partially from CNTs to Ni to form electron-rich nickel and increase the amount of nickel in alloying state, which promotes the catalytic activity of benzene hydrogenation [11]. That is to say, CNTs are acted as not only support in catalyst but also electronic catalyst-accelerator.

Table 1
Some characteristics of the samples determined by ICP and CO chemical adsorption

Catalysts	Ni loading (wt.%)	S_{Ni} ($m^2 g^{-1}$)
NiB/CNTs	6.64	32.9
NiB/γ-Al_2O_3	14.6	19.8

Table 2
Catalytic activity of benzene hydrogenation over different catalysts at different temperature (K)

Catalyst	Benzene conversion (mol%)					
	363	373	383	393	403	413
NiB/γ-Al_2O_3	35	45	59	70	81	90
NiB/CNTs	58	63	72	82	88	95

Table 3
The results of XPS

Binding energy (ev)	Sample ΔE (ev)		
	CNTs	NiB	NiB/CNTs
C 1s	284.05	284.35	+0.3
Ni $2p_{3/2}$	856.15	855.50	−0.65

Thermal stability is very important to amorphous alloy catalysts. How to improve the thermal stability of amorphous alloy catalysts has attracted more attentions for the purpose of using amorphous alloy in industrial process. In this paper, we also investigate the thermal stability of amorphous NiB/CNTs.

After NiB/CNTs and NiB/γ-Al_2O_3 catalysts have been reduced at 473 K, the temperature is increased to 673 K for 30 min to carry out thermal treatment on catalysts. Then the catalytic activities are evaluated under the temperature from 363 to 413 K, as shown in Table 4. The results show that the catalytic hydrogenation activity of both catalysts decreases obviously after thermal treatment, which shows amorphous alloy catalysts are sensible to high temperature. The catalytic activity of NiB/γ-Al_2O_3 decreases by 72.2% and that of NiB/CNTs decreases by 55% at 413 K, clearly showing that NiB/CNTs catalyst has better thermal stability.

The same conclusion can be drawn after analyzing DSC curves (see Fig. 1). There is one endothermic peak in the DSC curve of both NiB/CNTs and NiB/γ-Al_2O_3. The peak temperature is 335 and 370 K, respectively. This endothermic peak corresponds to the removing of ethanol or water in catalyst. The surface of CNTs is hydrophobic and the adsorbate is ethanol that is easier to vaporize than water. Hence

Table 4
Catalytic activity of benzene hydrogenation over different catalysts at different temperature (K) after thermal treatment

Catalyst	Benzene conversion (mol%)					
	363	373	383	393	403	413
NiB/γ-Al_2O_3	0	3.2	10	15	21	25
NiB/CNTs	17	19	25	28	33	43

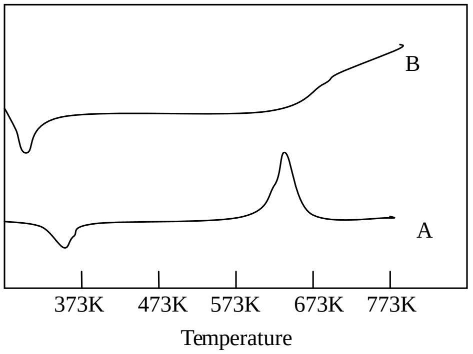

Fig. 1. The curves of DSC. A: NiB/γ-Al_2O_3; B: NiB/CNTs.

the endothermic peak temperature of amorphous NiB/CNTs is lower than that of NiB/γ-Al_2O_3. With the increasing of temperature, there is one exothermic peak appearing in the DSC curve of NiB/γ-Al_2O_3 catalyst. The peak temperature is 648 K that corresponds to the crystallization of amorphous alloy. Unexpectedly, there is no complete exothermic peak appearing in the DSC curve of NiB/CNTs catalyst. The peak starts to appear at about 663 K and does not have the tendency of falling down up to 773 K. The result shows amorphous NiB alloys supported on the CNTs start to crystallize at 663 K and this crystallization process does not end at 773 K. In order to find the reason, the NiB/CNTs catalyst is performed XRD measurement before and after being thermal-treated on the condition that is the same as that of the DSC measurement respectively. It can be seen from the XRD patterns (see Fig. 2) that the characteristic peak at $2\theta = 44°$ due to the metallic Ni is obviously broadened before thermal treatment. Thus, it can be concluded that the NiB alloy supported on CNTs retains typical amorphous structure before thermal treatment. After thermal treatment, the characteristic peak of Ni becomes sharper, implying the crystallization. However, the peak at $2\theta = 44°$ is broad-

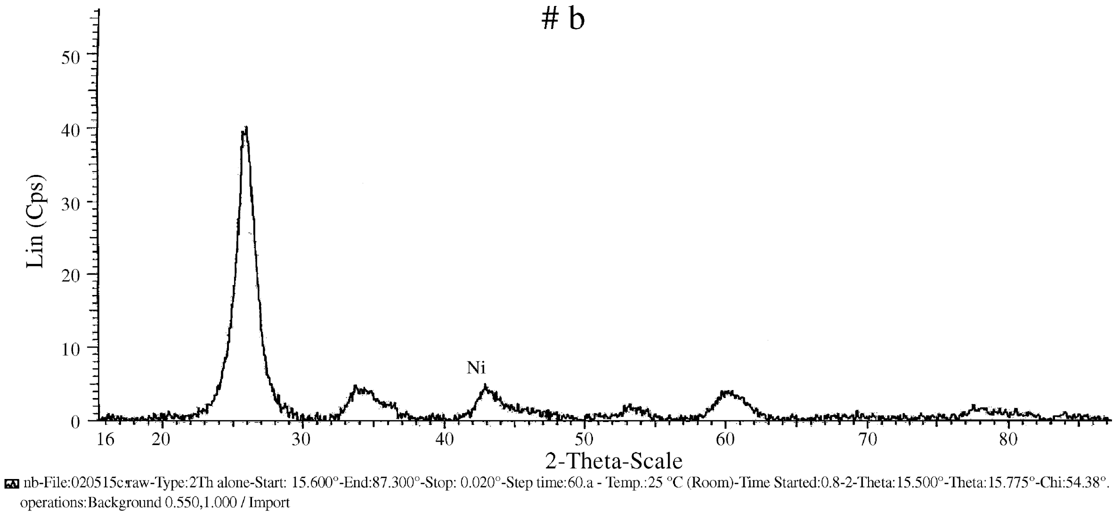

Before thermal treatment

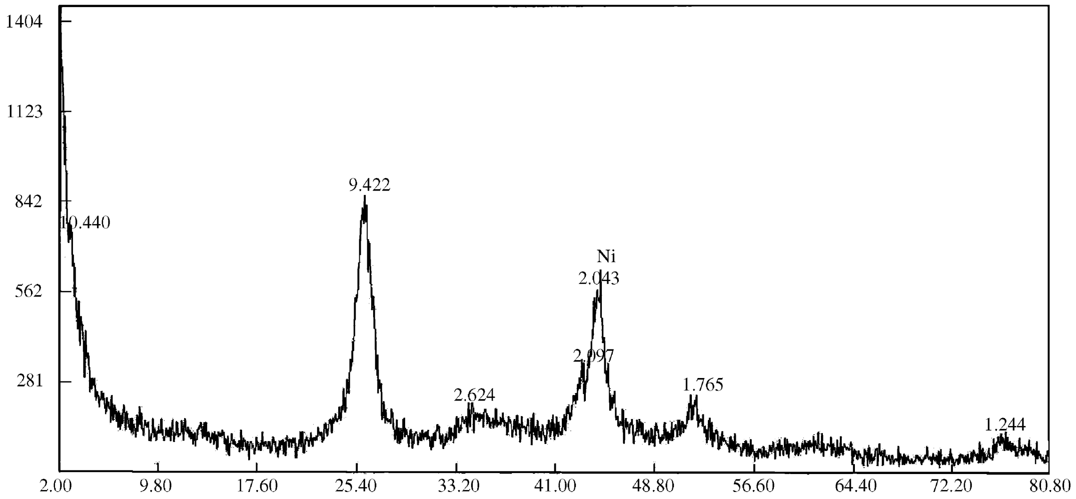

After thermal treatment

Fig. 2. The XRD patterns of NiB/CNTs.

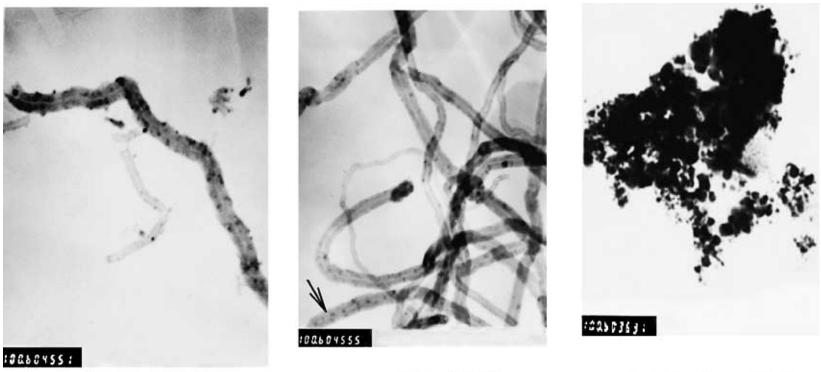

A: NiB/CNTs B: NiB/CNTs C: NiB/γ-Al_2O_3

Fig. 3. The TEM images.

ened to some extent while compared to the pattern of pure Ni crystalline hinting there are still some amorphous alloys existing in the catalyst after thermal treatment. From the TEM images (see Fig. 3A and B) of NiB/CNTs, we can find some components adhere to the exterior surface of CNTs and some exist in the inferior pore-channel as indicated by arrows. Therefore, it seems that with the increasing of temperature, the amorphous NiB particles adhering to the exterior surface of CNTs will aggregate and crystallize gradually, whereas NiB particles existing in the inferior pore-channel will not aggregate due to the restriction of pore size and still maintain the amorphous state. In additional, some conclusions can be drawn from Fig. 3 that CNTs, compared with γ-Al_2O_3, is in favor of the dispersion of amorphous NiB alloy, leading to the higher hydrogenation activity and thermal stability. This deduction is in accord with the results of DSC measurement and XRD measurement. That is to say, it is the unique central-hollow structure of CNTs that protects the active components against agglomeration and makes the active components maintain amorphous structure at higher temperature. This is beneficial for improving the thermal stability of amorphous NiB alloy supported on CNTs.

4. Conclusions

Amorphous NiB/CNTs and NiB/γ-Al_2O_3 catalysts were prepared by the impregnation combined with chemical reduction with KBH_4 aqueous solution. NiB/CNTs catalyst exhibited higher catalytic activity for benzene hydrogenation and better thermal stability than NiB/γ-Al_2O_3 catalyst because of the excellent electronic properties and the unique pore-channel structure of CNTs.

Acknowledgements

This work is financially supported by the National Natural Science Foundation of China and the Natural Science Fund of Jiangxi Province in China.

References

[1] R.B. Zhang, F.Y. Li, N. Zhang, et al., Appl. Catal. A: Gen. 239 (2003) 17.
[2] R.B. Zhang, F.Y. Li, Q.J. Shi, et al., Appl. Catal. A: Gen. 205 (2001) 279.
[3] S. Molnar, G.V. Smith, M. Bartok, Adv. Catal. 36 (1989) 329.
[4] J.F. Deng, H.X. Ling, W.J. Wang, Catal. Today 51 (1999) 113.
[5] N.M. Rodriguez, M.S. Kim, R.T. Barker, J. Phys. Chem. 98 (1994) 13108.
[6] Y. Zhang, H.B. Zhang, G.D. Lin, et al., Appl. Catal. A: Gen. 187 (1999) 213.
[7] H.B. Chen, J.D. Lin, Y. Cai, et al., Appl. Surf. Sci. 180 (2001) 328.
[8] P. Chen, X. Wu, J.D. Lin, et al., Science 285 (1999) 91.
[9] F.Y. Li, N.C. Peng, M.W. Wang, et al., Fenzi Cuihua 17 (2003) 65.
[10] P. Chen, H.B. Zhang, G.D. Lin, et al., J. Xiamen Univ. (science edition) 35 (1996) 61.
[11] S.H. Xie, H.X. Li, H. Li, et al., Appl. Catal. A: Gen. 189 (1999) 45.